

Supplementary figures

Supplementary figure 1

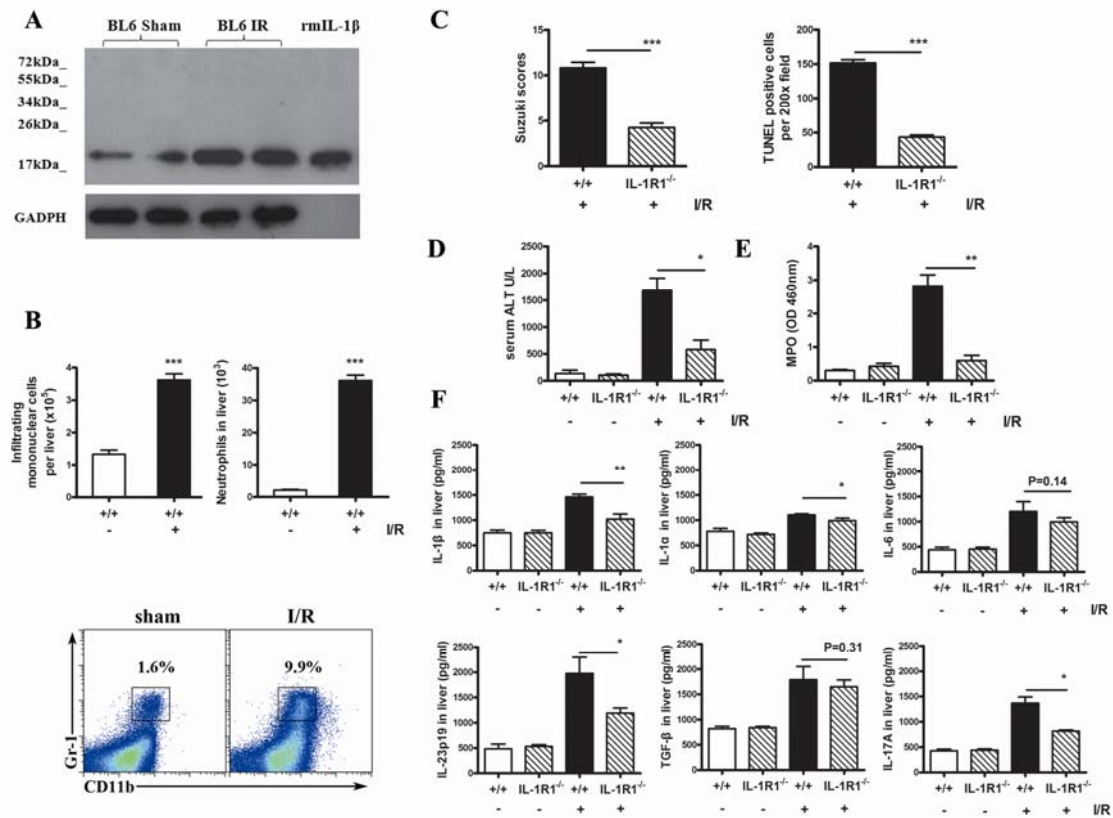


Figure S1. IL-1R1 deficient mice attenuated I/R injury and IL-17A expression

C57BL/6 mice and IL-1R1 deficient mice underwent I/R surgery or sham operation (white bar) and livers were collected 6h after reperfusion.

(A) Western blot analysis for hepatic IL-1β expression. (B) Total infiltrating leucocytes were isolated from livers, counted and further characterized as Gr-1^{hi}CD11b⁺ neutrophils by flow cytometry. (C) Hepatic I/R lesions from C57BL/6 and IL-1R1^{-/-} mice were graded using the Suzuki score. TUNEL positive cells were counted as described previously (200x). (D) Serum ALT level, (E) hepatic MPO activity from C57BL/6 and IL-1R1^{-/-} mice as compared to C57BL/6 mice following I/R and sham operation. (F) IL-1β, IL-1α, IL-6, IL-23/p19, TGF-β and IL-17A

protein levels in liver homogenate (ELISA). The data represent the mean \pm SEM (n=6-8 mice per group from three independent experiments, significant difference: * p < 0.05, ** p < 0.01).

Supplementary figure 2

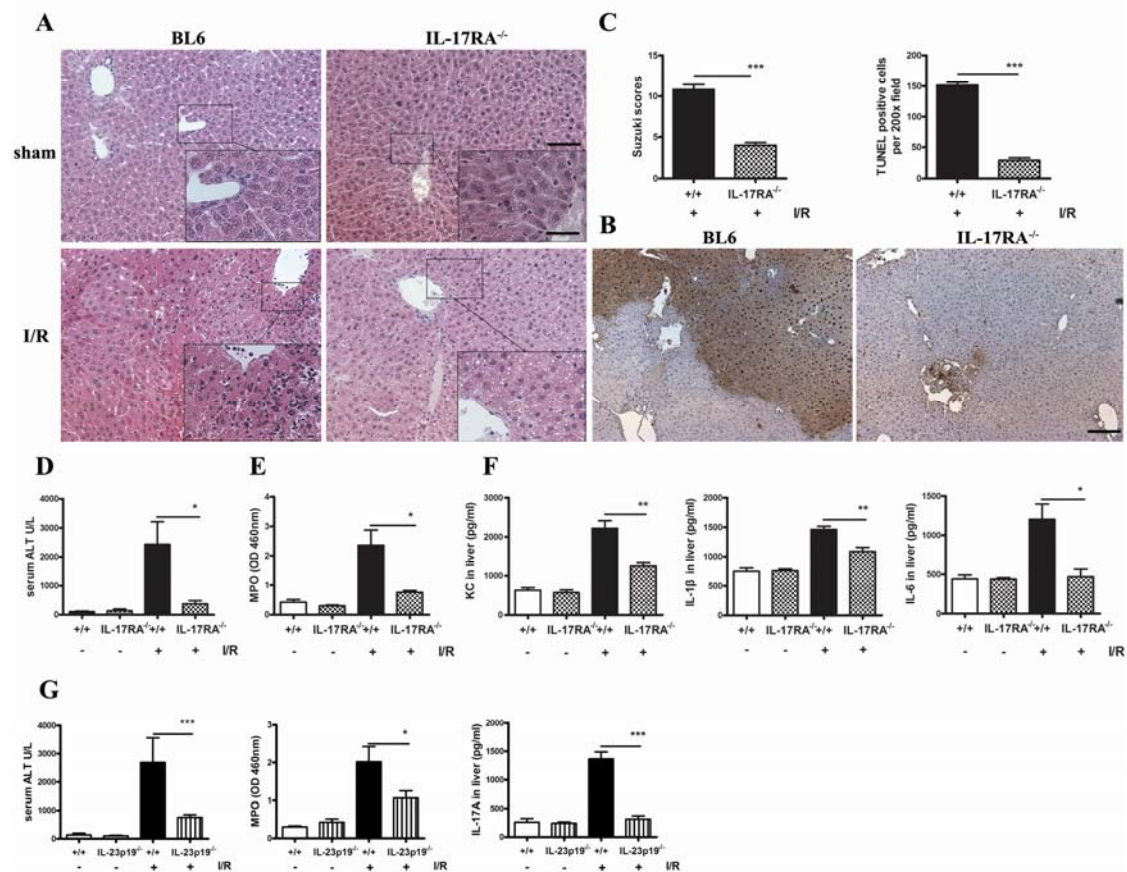


Figure S2. IL-17RA deficient mice are protected from hepatic I/R

IL-17RA^{-/-} mice and C57BL/6 mice were subjected to I/R or sham surgery as described before.

(A) Representative H&E (200x, 400x) and (B) TUNEL staining (200x) of liver from C57BL/6 and IL-17A^{-/-} mice subjected to I/R are shown. (C) Grading of I/R lesion were use the Suzuki scores and TUNEL positive cells were counted as described. (D)

Serum ALT levels, (E) hepatic neutrophil recruitment (MPO activity) (F). KC, IL-1 β and IL-6 from liver homogenates (ELISA) from C57BL/6 and IL-17RA^{-/-} mice which were subjected to I/R. The data represent as mean \pm SEM (n=6-8 mice per group from three independent experiments, * p < 0.05, ** p<0.01). (G) IL-23p19 knock-out mice subjected to I/R injury were measured for serum ALT activity, hepatic MPO activity and IL-17A concentration in tissue. The data represent the mean \pm SEM (n=6-8 mice per group from three independent experiments, significant difference:* p < 0.05, ** p<0.01).

Supplementary figure 3

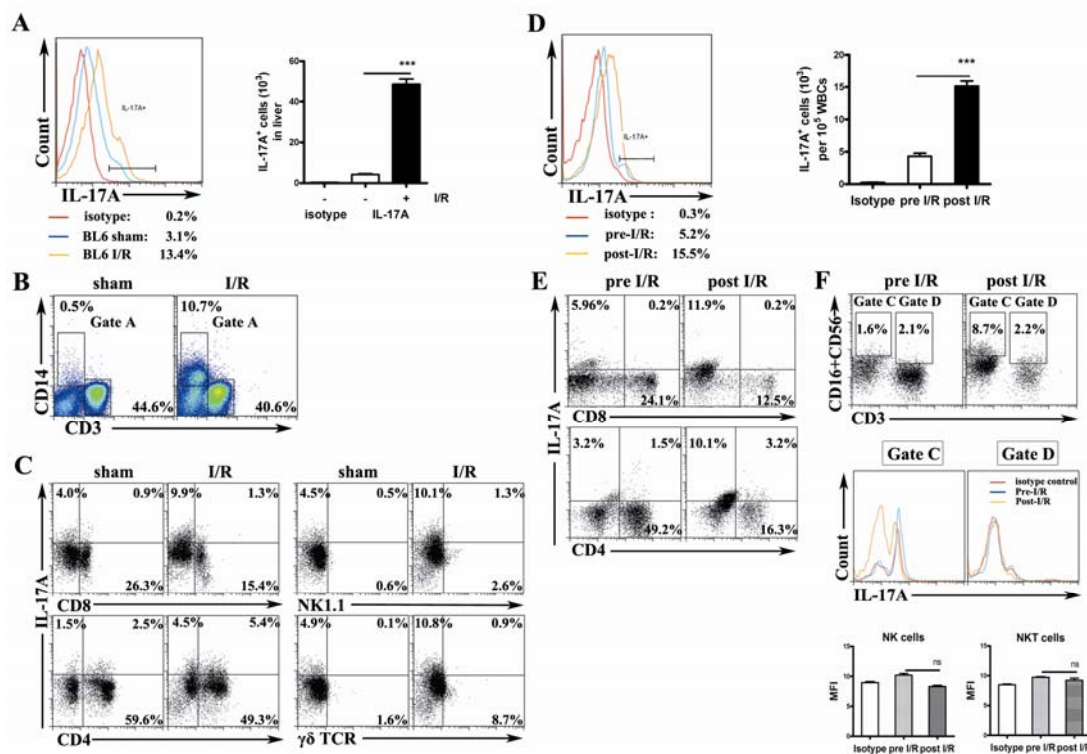


Figure S3. Neutrophils and CD4⁺ T cells are the main source of IL-17A in the liver upon I/R challenge in mice and human patients

Infiltrating mononuclear cells isolated from the mouse liver 6h after I/R and controls

(A-C). (A) Cells were permeabilized, stained by IL-17A specific antibodies and analyzed by FACS. Proportions and absolutely number of IL-17A positive cells are presented. (B) Analysis of CD3⁺ and CD14⁺ cells as described. (C) CD4⁺ T cells, CD8⁺ T cells, NKT and $\gamma\delta$ TCR⁺ cells were analyzed based on CD3⁺CD14⁻ gate. Results from one representative experiment of three independent studies (n=5 mice per group).

Investigations on PBMC from human patients following partial hepatectomy (D-F): (D) IL-17A staining histogram of PMA/ionomycin stimulated human PBMC (left panel), absolute numbers of IL-17A⁺ cells (right panel) from patients performed before and after partial hepatectomy. (E) CD4 and CD8 T cells were measured for IL-17A expression. (F) CD3⁺CD16⁺CD56⁺ or CD3⁻CD16⁺CD56⁺ measured by histogram and median fluorescence intensity to identify NK and NKT cells. Data are presented as MFI value \pm SEM. * (p<0.05; **, P<0.001, student t test). Results from flow cytometry are from one representative experiment of 7 independent studies.